# Examples of Using 3D-GPC-TREF for Polyolefin Characterization

*Wallace W. Yau*[*1,2]

**Summary:** Selected examples of using 3D-GPC-TREF to solve polyolefin characterization problems are described in this paper. The term 3D-GPC-TREF stands for a home-build hybrid system of gel permeation chromatograph (GPC) coupled with the capability of the temperature rising elution fractionation (TREF) that includes three online detectors, i.e. the infrared (IR), the differential-pressure viscometer (DP), and the light scattering (LS) detectors.

**Keywords:** polyolefin characterization; short-chain and long-chain branching; structure-property relations; triple-detector GPC; triple-detector TREF

## Introduction

A hybrid 3D-GPC-TREF system is built by installing a TREF add-on oil bath to an existing Waters 2000 CV GPC system[1] that has a built-in refractive index detector and a differential-pressure viscometer. Two additional detectors are added to the system; these are the Polymer ChAR IR4 dual-wavelength detector[2] and the PDI-1040 light scattering detector.[3] The Polymer Lab 20 micron mixed bed light scattering columns[4] are used in the GPC experiment. The configuration of the instrument is shown in the schematic in Figure 1. The six port valve in the system automatically switches the hot solvent flow through either the GPC or the TREF columns at several pre-determined time sequence steps. The column selection valve-switching is automatically synchronized with the oil bath temperature cooling and heating cycles in the TREF mode of operation. With the auto-sampler capability of the Waters 2000 CV system, up to 24 TREF samples can be loaded at one time and analyzed in an unattended operation at the rate of eight samples for every 24 hours. The TREF conditions for most of results reported in this paper are the following: the solvent is o-dichlorobenzene (ODCB) at 150 °C; the TREF column is packed with 27 micron glass beads; each three-hour TREF cycle consists of a 1.5 °C/min cooling step down to 25 °C followed by a 2 °C/min heating step back to 150 °C. The operation of this hybrid system has been reported in detail in two earlier publications.[5]

Polyolefin samples can have complex microstructures due to polymer branching and stereo-regularity differences. While the 3D-GPC experiment can be used to study polymer molecular weight distribution (MWD) and long-chain branching (LCB), the 3D-TREF experiment is needed to analyze polymer short-chain branching (SCB), co-monomer composition distribution (CCD), and the effect of stereo-regularity differences. For example, in a sample of Ziegler-Natta linear-low-density polyethylene (ZN-LLDPE), multiple TREF peaks are commonly observed that reflect the multiple-site nature of this catalyst type. However, the MWD curves of these ZN sites are broad and overlapping; therefore, they are not resolved in the 3D-GPC experiment. This is the value of using

[1] Equistar Chemicals, a Lyondell Company, 11530 Northlake Drive, Cincinnati, Ohio 45249 USA
E-mail: wallace.yau@equistarchem.com
[2] Present address: Characterization Group, Plastics R&D, B1470-D131, The Dow Chemical Company, 2301 Brazosport Blvd., Freeport, Texas 77541
E-mail: wyau@dow.com

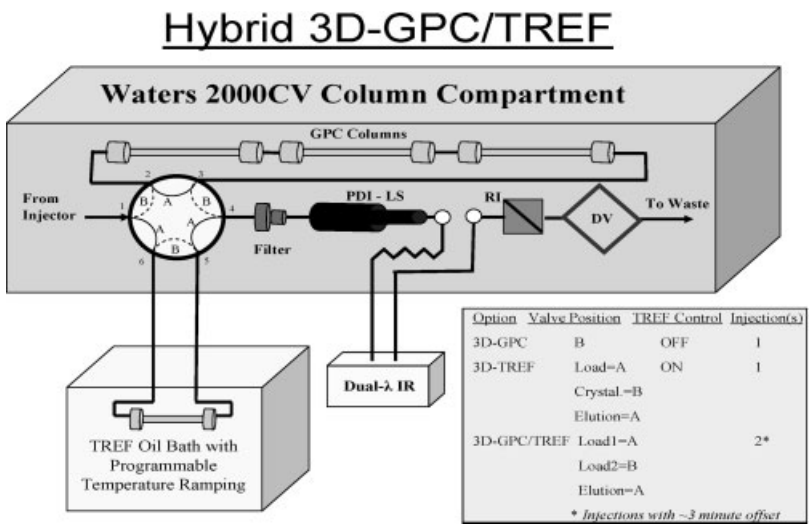


***Figure 1.***
Configuration of the hybrid 3D-GPC-TREF system.

GPC and TREF in a complementary way to analyze polyolefins for greatly improving the understanding of their complex structures.

One way to explain the complex multiple-site nature of polyolefin structures is to visualize it in a three-dimensional picture, as shown in Figure 2. In this illustrative model of a ZN-LLDPE sample, we can explain the structural features seen by GPC versus those seen by TREF. When viewing the graph in the GPC direction (bottom left frame), one sees the result of the overlapping MWD profiles of the multiple sites that are stacked together with one behind

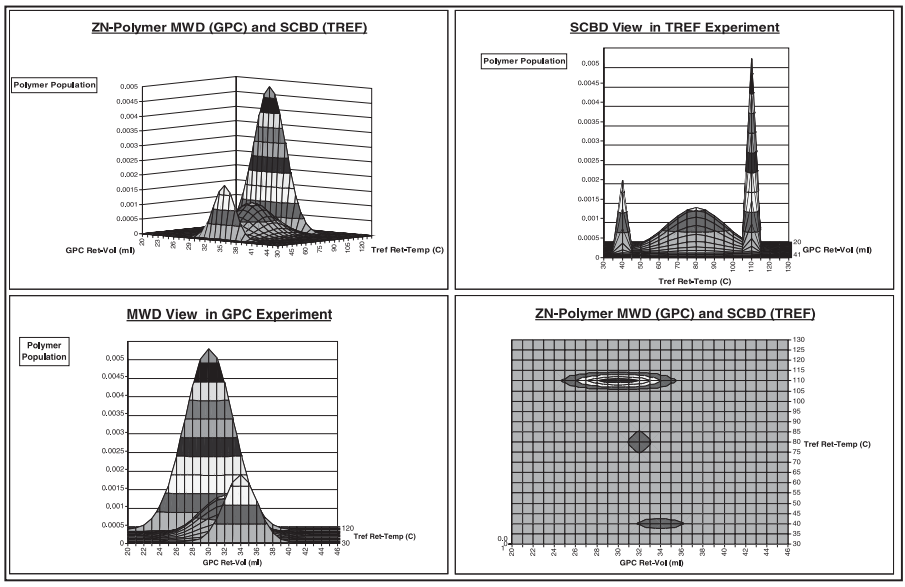


***Figure 2.***
A three-dimension illustration of the complex nature of polymer $\mu$-structure.

 

the other. Only in the TREF view (top right frame) can one see the resolution of the multiple-site populations in the polymer structure. Viewing from the top (bottom right frame), one sees the three-dimensional aspect of the polymer structure.

In the study examples presented in the next section, we will see the synergistic value of combining the 3D-GPC and the 3D-TREF results in solving polymer characterization problems. In some cases, we show a single ''polymer $\mu$-structure'' plot made up by the side-by-side display of the results from 3D-GPC and 3D-TREF. The term ''polymer $\mu$-structure'' is used in reference to the molecular structural features of polymer that include MW, MWD, SCB, LCB, and CCD.

## Study Examples

There are many unique features and capabilities of the 3D-GPC-TREF technique useful for supporting all functions in a polyolefin R&D program. They have been used to solve problems in catalyst research, pilot plant and product development trials, tech-service and customer complaints, and competitive product analyses. A selective number of examples of such studies are presented below.

### High Precision Detection of Subtle Polymer Structural Differences

In an effort to develop a LLDPE product to qualify for a stretch film application, some level of LCB detrimental to film performance was detected by 3D-GPC as shown in Figure 3. The level of LCB can be quantified by the size of the high molecular weight hump in the LS curves. The result shows that the LCB is much less in the two competitor products. It is plausible that this unexpected LCB in the current product might be the result of the melt extrusion process used to produce polymer pellets. To answer this question, tests were done on a sample of the reactor powder as well as on the pellets made from the powder. The small LCB difference between the pellet and powder seen in Figure 3 clearly shows that the melt extrusion process could not be the culprit of the LCB problem. This result helped direct attention to the reactor kinetics and catalyst preparation to solve the problem. This example is selected to emphasize the importance of the high precision quality of the polymer analysis data in solving real life problems.

Another example for the need of high precision data is the study of peroxide type in a low-density polyethylene (LDPE) process. As shown in Figure 4, the differences made by peroxide change are very

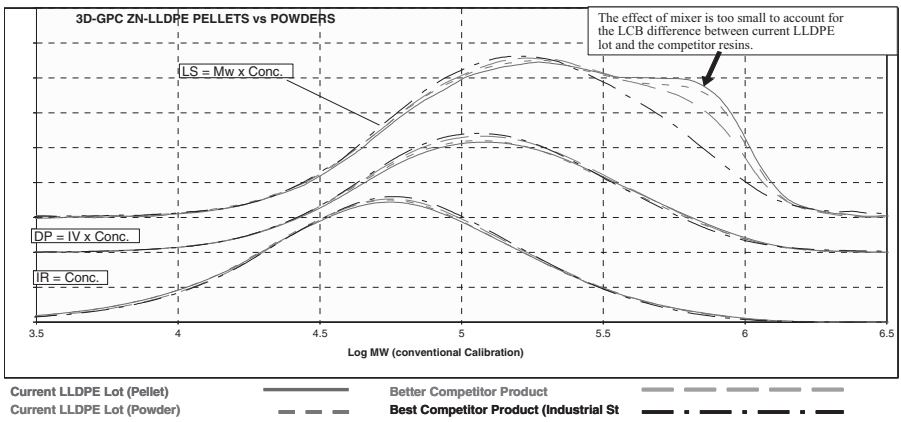


***Figure 3.***
High precision detection of LCB in ZN-LLDPE.

 

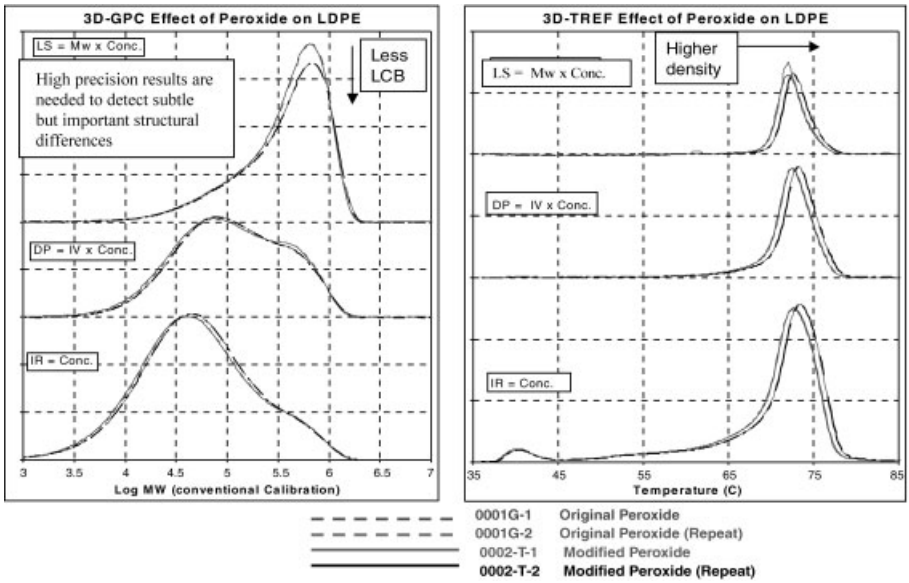


***Figure 4.***
High-precision 3D-GPC-TREF study of peroxide effect on LDPE production.

small, but they were clearly recognizable in our 3D-GPC-TREF results. These subtle LCB differences would not have been revealed so clearly without the high precision features of our 3D-GPC-TREF instrument. The good repeatability of our instrument is shown by the results of repeat sample analyses in Figure 4. These differences in LCB and product density as detected by 3D-GPC-TREF are very small, but they are responsible for significant differences in polymer end-use properties. Great emphasis was made in our home-made 3D-GPC-TREF system with many built-in automated control features to maximize the repeatability of sample analyses.

### LCB Detection in 3D-GPC-TREF

As demonstrated in Figure 3 and 4, the effect of LCB can be seen qualitatively by visual inspection of the 3D-GPC or 3D-TREF curves. However, in order to quantify the LCB level more precisely, we have introduced two LCB indices to process the data, as described in Figure 5 and 6. The formulations of these two new LCB indices (gpcBR and trefBR)[6] are created in a way that they can be used for direct comparison with the LCB index (LCBI) used in the rheological tests.[7] The definition of gpcBR and trefBR takes advantage of the four most precisely measured parameters in the 3D-GPC-TREF experiments, i.e., the LS-measured $M_w$, the viscometer-measured IV, and the conventional GPC-measured $M_w$ and $M_v$ values, where $M_w$, IV, and $M_v$ stand for the weight-average molecular weight, intrinsic viscosity, and viscosity-average molecular weight, respectively. The calculated gpcBR and trefBR values represent the average LCB level in the bulk sample.

The calculated gpcBR and trefBR values are included in the final report of every 3D-GPC-TREF analysis. An example of such a report is shown in Figure 7 and 8 for the comparison of a tubular versus an autoclave LDPE sample. It is commonly observed that the tubular LDPE has higher density (higher TREF elution temperature) and lower LCB (lower gpcBR and trefBR values) than its autoclave LDPE counterpart.

The value of the combined information from 3D-GPC and 3D-TREF serves nicely for the purpose of answering a usual question of ''gel'' or ''un-melt,'' a problem

 

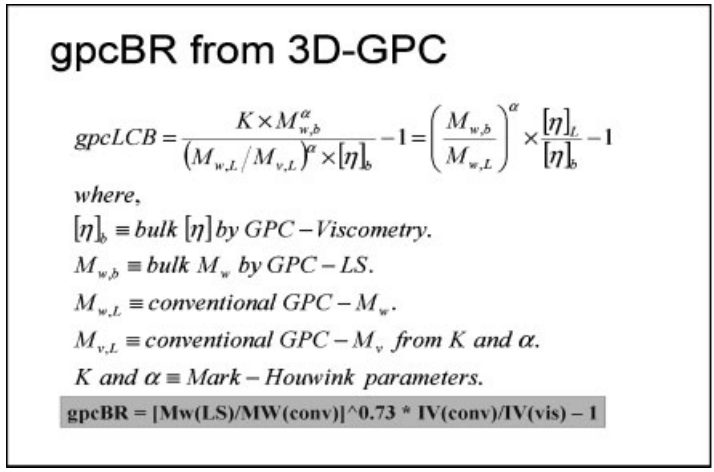


***Figure 5.***
High-precision LCB index gpcBR by 3D-GPC.

often encountered in thin films of high-density polyethylene (HDPE). The results of one of these studies are shown in the $\mu$-structure plot in Figure 9, where the results of the ''gel'' particle are being compared with the results of the clear HDPE film base that contains no ''gel.'' Here, the 3D-GPC side of the plot shows the structure being mainly of a linear high molecular weight material with no significant LCB. This observation is derived from the fact that the size of viscosity peak also increases along with the increase in the LS peak. *The presence of LCB would increase the viscometer peak to a lesser extent than the LS peak*. The 3D-TREF side of the plot shows the structure being mainly of the high melting type, just like the HDPE film base, with no indication of significant branching structure. These results are indicative of the problem being more of a high molecular weight ''un-melt'' rather than that of a ''gel'' or cross-linking branching problem in the usual sense. Because a very limited amount of the ''gel'' particles can be extracted from a film sample, the very small

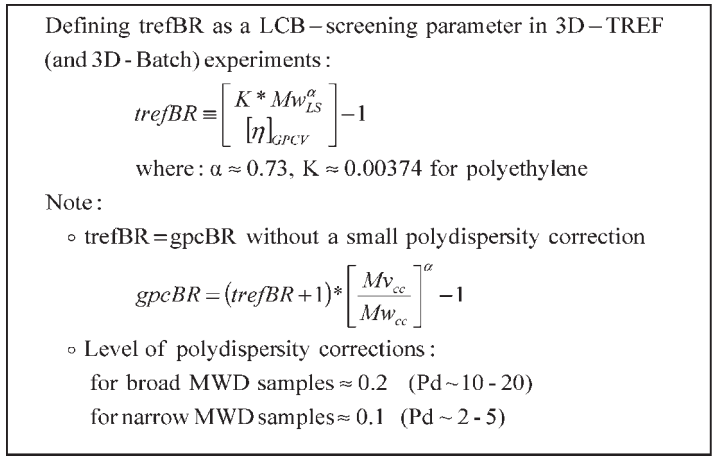


***Figure 6.***
High-precision LCB index trefBR by 3D-TREF.

 

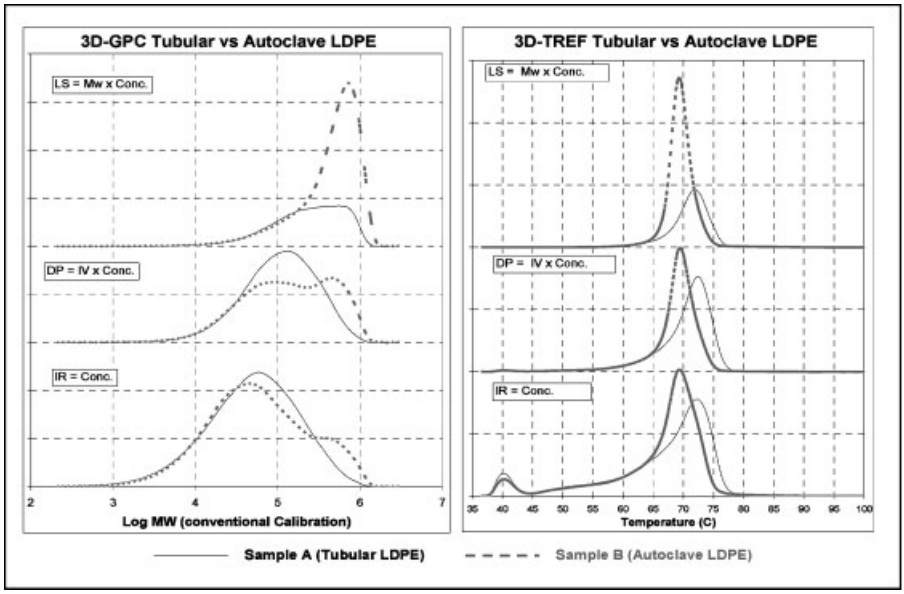


***Figure 7.***
The 3D-GPC-TREF $\mu$-structure plot for tubular versus autoclave LDPE.

**3D-GPC Summary**

*Job :* Tubular vs Autoclave LDPE — *Machine :* GPC-xxx

| Sample Num | Sample-A | M bulk | Mz+1 | MLS/MCC | MLS/MNCC | IV bulk | g-prime | gpcBR |
|---|---|---|---|---|---|---|---|---|
| Product # | Tubular LDPE | 190,404 | 574,868 | 1.943 | 10.116 | 0.928 | 0.656 | 1.477 |
| | | Mp | Mn | Mw | Mz | D | % < $10^4$ | % > $10^6$ |
| | | 57,123 | 18,822 | 97,988 | 340,729 | 5.21 | 11.39 | 0.09 |
| Sample Num | Sample-B | M bulk | Mz+1 | MLS/MCC | MLS/MNCC | IV bulk | g-prime | gpcBR |
| Product # | Autoclave LDPE | 423,612 | 753,307 | 3.021 | 21.022 | 0.887 | 0.501 | 3.472 |
| | | Mp | Mn | Mw | Mz | D | % < 104 | % > 106 |
| | | 45,322 | 20,150 | 140,227 | 548,847 | 6.96 | 10.61 | 0.83 |

**3D-TREF Summary Report**

*Job :* Tubular vs Autoclave LDPE

| SM No. / Sample ID / Lot No. | Zone-1 Solubles @ 40°C | | | Zone-2 Polymer 40°C < Temp <110°C | | | trefBR=K*Mw^0.73/IV-1 K=0.000374 for PE |
|---|---|---|---|---|---|---|---|
| | Wt. % | Cal'd Mv | IV g/dl | Wt. % | Cal'd Mv | IV g/dl | Remarks |
| Sampe A Tubular LDPE | 7.0% | 5,000 | 0.17 | 93% | 197,000 | 1.03 | |
| | | | | | trefBR = | 1.66 | |
| Sampe B Autoclave LDPE | 5.0% | 14,000 | 0.16 | 95% | 403,000 | 0.98 | Autoclave LDPE has higher LCB and lower TREF elution temperature. |
| | | | | | trefBR = | 3.72 | |

***Figure 8.***
3D-GPC-TREF summary report for tubular versus autoclave LDPE.

 

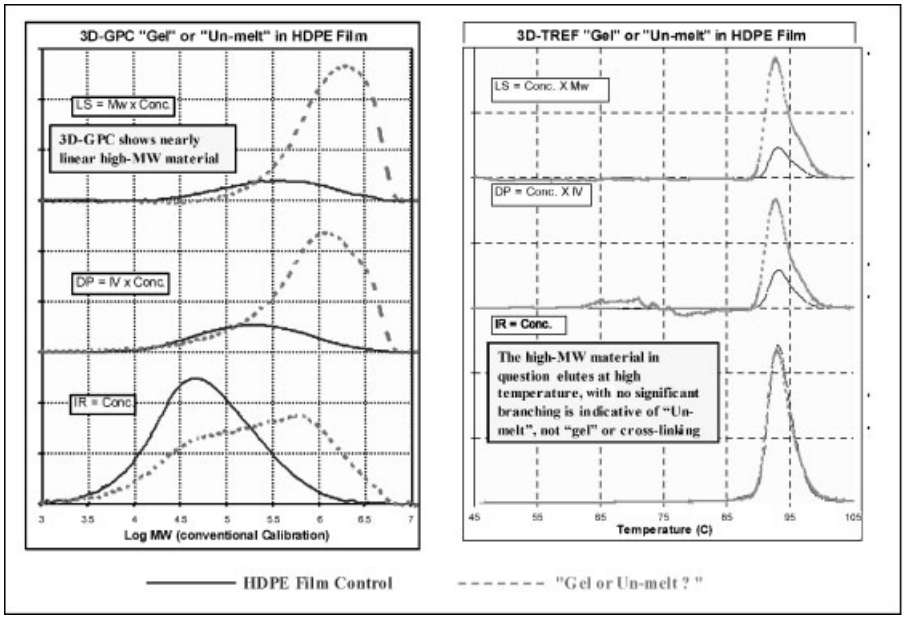


***Figure 9.***
3D-GPC-TREF determination of "gel or un-melt?" structure in HDPE film.

sample sizes makes it very difficult for them to be studied by most other analytical tests. This makes 3D-GPC-TREF uniquely useful for samples as little as a fraction of a milligram. Highly cross-linked gels may exist in samples that may not dissolve in hot TCB. These gel structures would not be injected in either the GPC or TREF column, and would not be detected. The presence of these gel fractions can be estimated by the percent mass recovery data in the GPC or TREF experiment.

In the next study example, we show that one can distinguish different types of LCB in polymers and that LCB is not limited to LDPE. LCB can exist in HDPE made from ZN slurry process or as a result of thermal degradation and chain extension processes in melt extrusion. While the 3D-GPC side of the $\mu$-structure plot in Figure 10 shows the existence of LCB in all three samples, 3D-GPC is not capable of distinguishing the LCB types. However, the LCB in LDPE is clearly distinguished from that in the HDPE samples by the 3D-TREF result shown in Figure 10. The two HDPE samples with LCB content elute from TREF at high temperature, but the LDPE sample has a lower TREF elution temperature because of its high content of butyl (C4) branching. *These C4 branches are the result of the chain-end backbiting branching mechanism in the high-pressure LDPE process. It is kind of fascinating to picture that the basic structure of LDPE minus the presence of LCB would not be very different from a single-site hexene LLDPE copolymer of very narrow CCD.*

## Moderation of Co-Crystallization Effect in TREF Separation

Co-Crystallization of polymer blends is a complicating factor that can compromise the accuracy of the compositional analyses by TREF and by crystallization analysis fractionation (Crystaf).[8] Strong co-crystallization distorts the elution profile of TREF and Crystaf separations. Evidence has been reported that the co-crystallization problem is less severe in TREF than in Crystaf. These reports conclude that TREF is more appropriate for analyzing samples with complex CCDs because it provides better peak resolution of blends. Nevertheless,

 

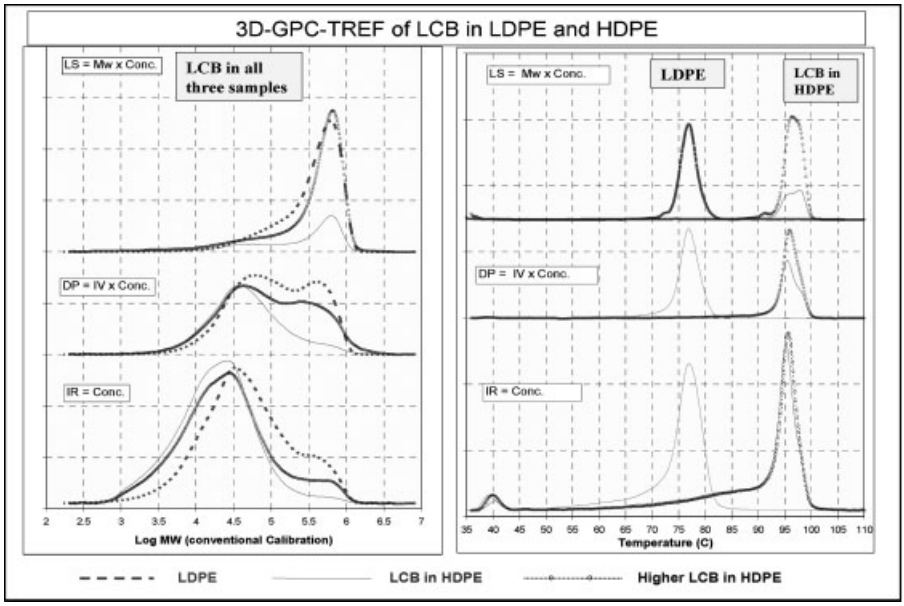


***Figure 10.***
LCB in LDPE versus LCB in HDPE.

co-crystallization still is a concern in fast TREF separations using fast cooling rates.

In our study reported below, we have managed to reduce the co-crystallization effect in TREF by using glass bead packing instead of polymeric di-vinyl benzene (DVB) packing. Reasonable control of the co-crystallization effect has been made possible even at fast TREF analyses at the rate of three to four hours per sample. The results of this study are explained in Figure 11 and 12 for the DVB and glass bead TREF columns, respectively. (The glass beads GL-0191 of 18–27 microns were purchased from MO-SCI Specialty Products, LLD, 4000 Enterprise Dr., Rolla,

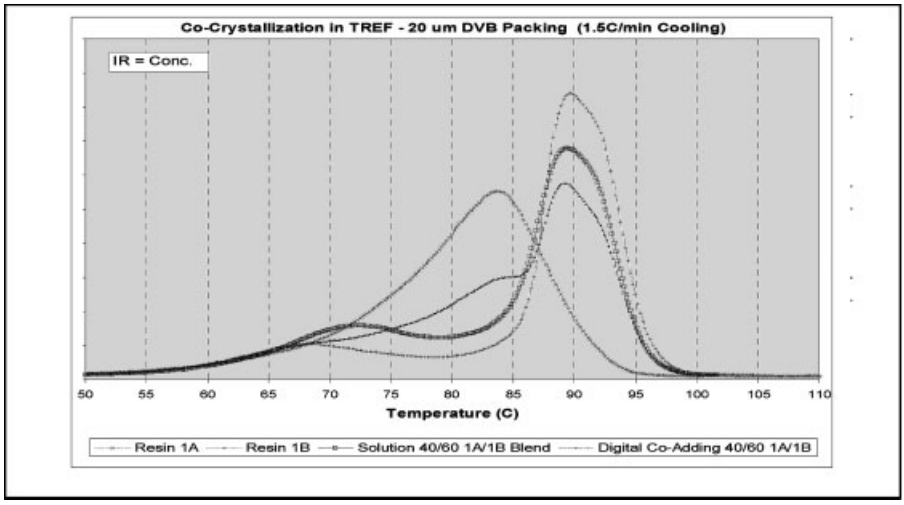


***Figure 11.***
Strong co-crystallization effect in a TREF column with DVB packing in a 3-hour TREF experiment.

 

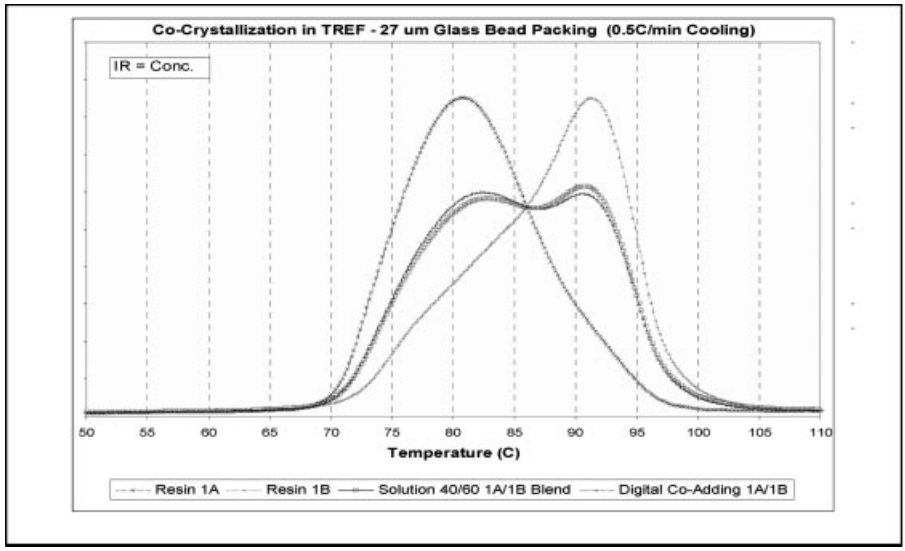


***Figure 12.***
Minor co-crystallization effect in a TREF column with glass bead packing in a 4-hour TREF experiment.

MO 65402.) In each figure, there are three experimental TREF elution curves: one for each of the two components in the blend and a third curve for a solution blend sample of the two components. The fourth curve in each figure is the digitally co-added results of the two component curves.

The difference between the curve of solution blend and the co-added curve provides the measure of the co-crystallization effect. It is clear that co-crystallization effect is much worse with the DVB packing in Figure 11 than for the glass bead TREF column in Figure 12. The cooling rate is found to have an effect on the degree of co-crystallization, but only to a much lesser extent than the effect caused by the difference of the TREF packing material. It is clear that, under proper TREF conditions, the co-crystallization problem can be moderated considerably as shown in Figure 12, which gives still reasonably short TREF analyses at the rate of four hours per sample.

### Analyses of Resin Compositions in A Multi-Layer Polymer Film

Under the TREF conditions without strong co-crystallization, the 3D-TREF technique can be used to study the compositions of polymer blends or components in the multi-layer films. In the example study below, we were asked to find out the resin compositions in an unknown polymer film. We were provided with five resin samples that might have been used in making the film. To approach this problem, we first obtained the 3D-TREF results for the film and the five resins. We then used the Excel solver program to search for the answer. The results are explained below with the help of Figure 13 and 14 for the raw 3D-TREF data and the solver search results, respectively.

The top row in Figure 13 shows the IR, DP and LS profiles of the TREF runs for the unknown film sample. The bottom row shows the corresponding detector tracings of the TREF runs for the five resin samples. The 3D-TREF curves of the five resins are consistent with the following polymer types: 1 = an isotactic polypropylene (iPP), 2 = a metallocene LLDPE (mLLDPE), 3 = a ZN-LLDPE, 4 = a second mLLDPE, and 5 = a plastomer. The first thing we observed was that resins 2 and 4 had identical 3D-TREF profiles. They are likely the same mLLDPE product.

The goal of the study was to find the best combination of the TREF curves for these

 

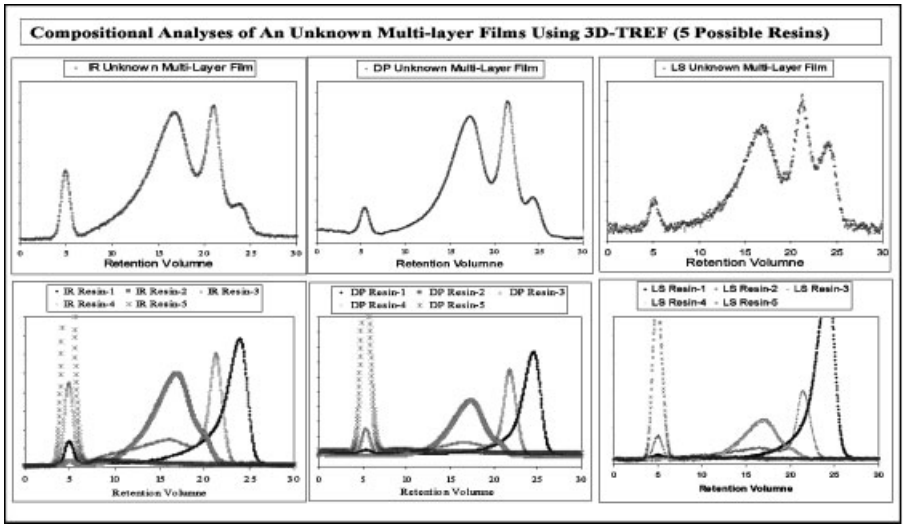


***Figure 13.***
Raw 3D-TREF data of an unknown multi-layer film and the five possible resin components.

resins to match those of the unknown film sample in each of the three detector signals. This was quite a curve-fitting challenge that would not have been possible without the help of a curve-fitting program like the Excel Solver. The Solver search results, shown in Figure 14, indicate that the film was made up by three resin components – iPP, mLLD, and a ZN-LLD – with the estimated weight percentage of 10, 40, and 50%, respectively. The co-added curve from this three-resin combination for each detector is shown in Figure 14 and compared with the 3D-TREF data of the

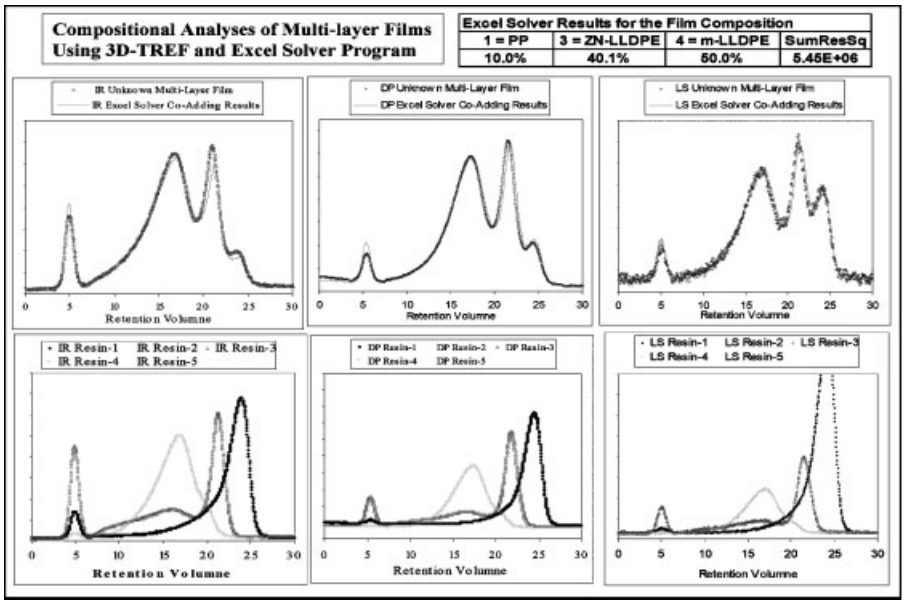


***Figure 14.***
Use of 3D-TREF and Excel Solver for the compositional analysis of a multi-layer film.

 

unknown film sample. We were pleasantly surprised to see the very good fit between the predicted and the experimental data for the film sample. With the success of this study, it is possible to say that under favorable conditions, the 3D-TREF can be quite useful for quantitative studies of polymer blends and can be used as a tool for the compositional reverse-engineering of fabricated products.

### Characterization of Reverse MW-SCB Dependency

Comonomer incorporation is a very important practice for optimizing the properties of LLDPE and HDPE products. It is highly desirable to have the comonomers distributed more in the higher molecular weight fractions of the sample to achieve a greater effect of the comonomer presence to the polymer property. For catalysis research and product development, there is a strong need for analytical techniques that can determine the molecular weight dependency of comonomer and SCB distribution in polymer products. One approach has been reported with the use of an online Fourier transform IR detector (FTIR) in a GPC experiment.[9] However, in a rather roundabout way, some aspect of the polymer MW-SCB dependency can also be determined by the 3D-TREF method. This can be explained with the help of the sketches shown in Figure 15 and 16.

Figure 15 depicts a GPC experiment where a ZN-LLDPE sample is separated across the MWD in the x-direction. The downward pointed wide-arrow in the middle of the Figure is an illustration for this ZN-type MW-SCB dependency, i.e., the SCB (or co-monomer content) decreases with increasing molecular weight. What researchers wish to achieve is the reversed MW-SCB dependency in the product, i.e., the MW-SCB trend depicted by the upward pointed wide-arrow in the Figure. The nature of the MW-SCB analyses is obviously a two-dimensional problem. We need comonomer detection (e.g. FTIR) in the y-direction to complement the GPC-MWD information in the x-direction. This is how the GPC-FTIR method works. *Alternatively, one can also get the SCBD information by a cross-fraction of GPC fractions by a second TREF analysis, as depicted on the left y-axis of the sketch. This would be called a GPC-TREF cross-fractionation.*

To explain how 3D-TREF works to determine MW-SCB dependency, we turn the GPC-based sketch in Figure 15 into the TREF-based sketch in Figure 16 by a 90° rotation of the plot. In this case, we now

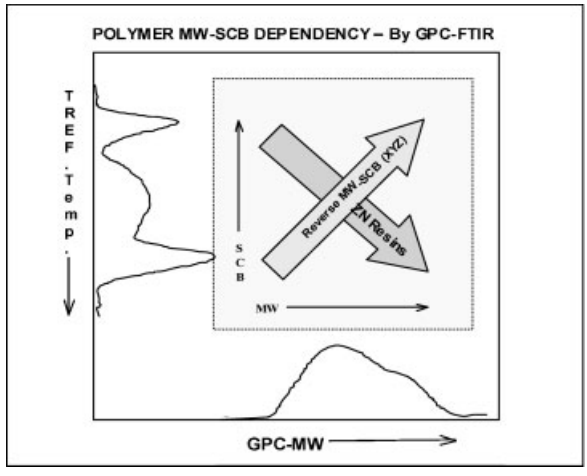


***Figure 15.***
A sketch to explain the determination of polymer MW-SCB dependency by GPC-FTIR analysis.

 

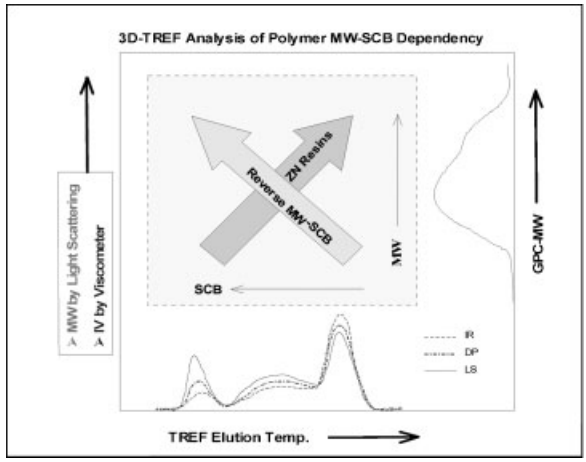


***Figure 16.***
A sketch to explain the determination of polymer MW-SCB dependency by 3D-TREF analysis.

have the SCB and comonomer content information displayed across the x-direction. The wide-arrows for the ZN and reversed molecular weight dependency are still in place to show the desired information we try to determine. What is needed in this case is the molecular weight information in the y-direction. This need is met obviously by the LS-$M_w$ and Viscometer-IV information derived from the triple-detector features of the 3D-TREF technique. *If GPC is used to get the MWD information of the TREF fractions, this situation of course becomes the technique known as the TREF-GPC cross fractionation.*

An example of a typical 3D-TREF report on polymer MW-SCB dependency is shown in Figure 17 for two LLDPE samples: one is a ZN type and the other is of the reversed MW-SCB type produced with a mixed metallocene catalyst. To help the visualization of the relative molecular weight dependency across the TREF curves, the 3D-TREF curves in this figure are plotted in the so-called ''relative-scale'' mode, where the three detector signals are normalized to the same height at the peak of the highest IR peak. In this plot option, the relative molecular weight and IV trend in the three temperature zones can easily be recognized visually. Typically, we report the results in three zones, i.e., the ''soluble fraction'' zone 1, the ''high-impact'' zone 2, and ''homopolymer fraction'' zone 3. The elution temperature limits of these zones can be varied to fit the specific need of the 3D-TREF study. If needed, reporting the results in more number of temperature zones can be easily accommodated. In the example shown in Figure 17, these three zones are chosen to be the soluble fraction that elutes below the temperature of 40 °C, zone 2 of elution temperature between 40 °C and 85 °C, and zone 3 for fractions at elution temperatures higher than 85 °C.

For sample A of the ZN-LLDPE type shown at the upper left corner of Figure 17, we see first that the multiple TREF peaks reflecting the multiple sites are clearly separated. Second, we see that the LS signal decreases toward the lower-melting fractions. That means that the comonomer fraction is higher in the lower molecular weight chains in zone 2. This is a MW-SCB trend that is opposite to what a researcher would have wished to make. On the other hand, for sample B from a mixed mLLDPE catalyst, we see that LS signal is higher for the lower melting peak of higher comonomer content. This gives a clear indication that the comonomer fraction is indeed higher in the higher molecular weight

 

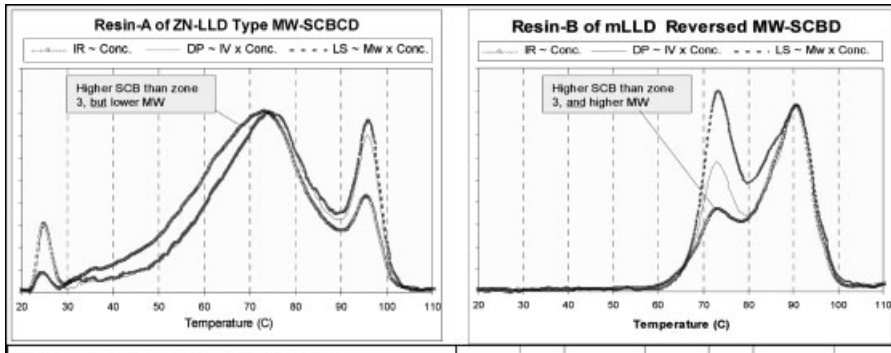


**3D-TREF Study of the MW-SCB Dependency**

| SM No. Sample ID Lot No. | Zone-1 Solubles Temp < 40°C | | | Zone-2 Low-Melts 40°C < Temp <85°C | | | Zone-3 High-Melts 85°C < Temp < 120°C | | | Ratio Zone2 / Zone3 | | |
|---|---|---|---|---|---|---|---|---|---|---|---|---|
| | Wt. % | Mw | IV g/dl | Wt. % | Mw | IV g/dl | Wt. % | Mw | IV g/dl | Wt. % | Mw | IV g/dl |
| Resin-A ZN-LLD | 13.7% | 63,000 | 0.72 | 66% | 107,000 | 1.41 | 20% | 174,000 | 2.17 | 3.32 | 0.61 | 0.65 |
| Resin-B mLLD Reversed MW-SCBD | 0.0% | ~ | ~ | 46% | 108,000 | 1.04 | 54% | 67,700 | 0.89 | 0.85 | 1.60 | 1.18 |

***Figure 17.***
Quantification of the reverse MW-SCB dependency of LLDPE samples.

chains in this sample, as one would have hoped to achieve in catalyst research. To quantify this reversed MW-SCB dependency, we process the TREF results in the three zones to provide the values of weight percentage, $M_w$, and IV in each zone. The results of such calculations are shown in the bottom table of Figure 17. The ratio of the $M_w$ and IV values between zone 2 and zone 3 is also reported in the last column of the table. The degree of reversed MW-SCB dependency can therefore be quantified by theses ratio values. The level of reverse MW-SCB dependency is proportional to how much higher the molecular weight ratio exceeds the value of 1.0. Therefore, the reversed MW-SCB dependency in sample B is reflected in the high molecular weight ratio of 1.60, while the value is 0.61 and less than one for sample A of ZN-LLDPE type.

The molecular weight and the amount of the soluble fraction, *or the lack of it*, are important pieces of information of the samples as well, especially for studying high-impact polypropylene, thermoplastic olefin (TPO) and tie-layer products that depend on the solid state rubbery-versus-crystalline phase separation in their end-use applications. Some examples for such applications are presented below.

**Structural Studies of Functional Polyolefin**

The value of the sub-ambient TREF capability of our instrument using ODCB solvent is demonstrated in the study example of the two commercial tie-layer products shown in Figure 18. The rubber phase components in the two products both elute as the ''soluble fractions'' in the 25 °C TREF experiment shown in the top two curves. The important compositional difference of the rubber components used in the two products can only be revealed in the sub-ambient 0 °C TREF experiment shown in the two bottom curves.

Good use can be made of the dual-wavelength feature of the IR4 detector in our 3D-GPC-TREF system. One wavelength (IR1) in this detector has comparable detection sensitivity for both the aliphatic methylene ($CH_2$) and methyl

 

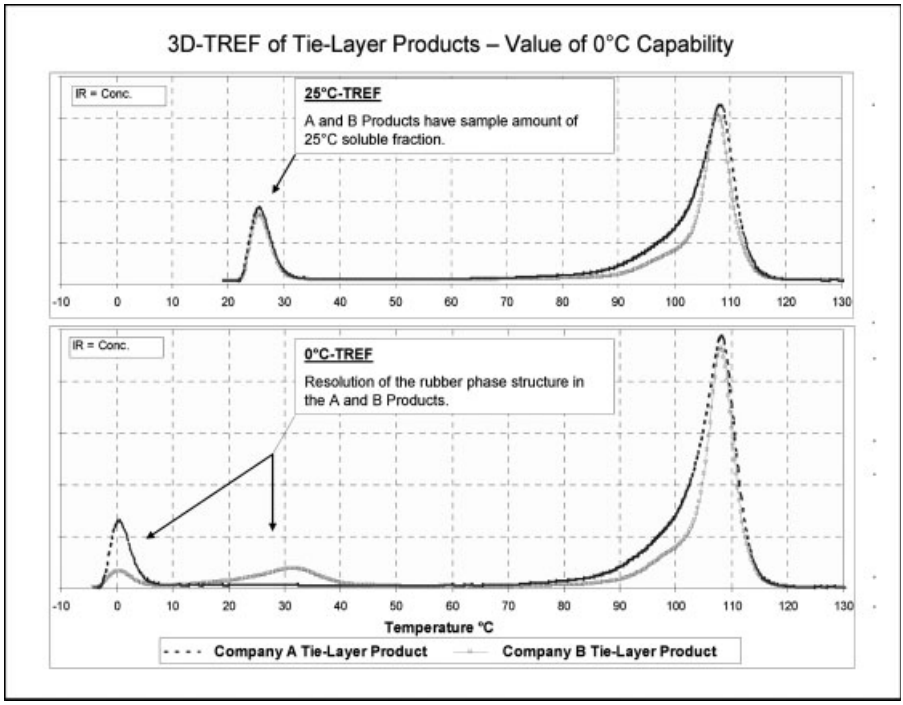


***Figure 18.***
Value of sub-ambient TREF capability for the compositional study of the rubber phase components in tie-layer products.

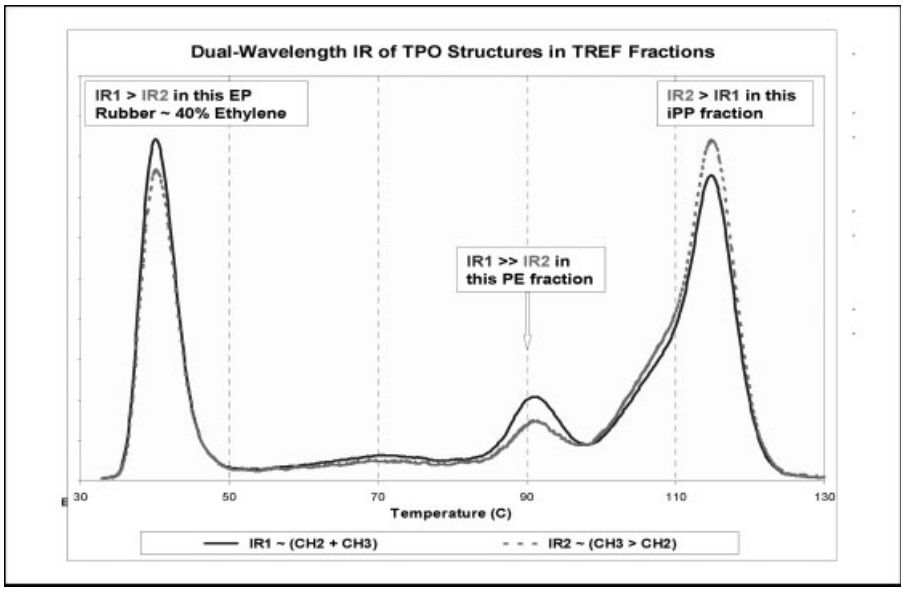


***Figure 19.***
Dual-wavelength IR detection of TPO structures in TREF fractions.

 

($CH_3$) groups in polyolefins, while the 2nd wavelength (IR2) is more sensitive for detecting $CH_3$ than the IR1 wavelength. An example of the dual-wavelength IR application is shown in Figure 19 for a TREF study of a polypropylene-based TPO sample. With the presence of both IR1 and IR2 detector signals, one can see the ethylene-propylene compositional differences across the TREF curve by observing the relative peak heights between the IR1 and IR2 signals. By doing so, one can easily identify the structure of the three main peaks in the TREF curve as the following: a large isotactic polypropylene component at high-melting, a small HDPE peak near 90 °C and a large EP copolymer rubber component in the soluble fraction peak.

In the study example below, the effect of visbreaking on HDPE was studied with and without a functional modifier. The results are shown in Figure 20. Under the condition of no modifier, one sees only the effect of the chain scission effect of the visbreaking process. In this case, we see a decrease in molecular weight (lower LS signal) of the product as compared to the starting HDPE material. The visbroken product in this case still has the microstructure of a HDPE, as indicated by the fact that the TREF peak remains at the same high elution temperature position. For the case where a functional modifier is included in the visbreaking process, one sees that there is an additional shift of resulting material to a lower TREF elution temperature. This observation of the down shift in elution temperature is of value to learn about how the modifier molecules are incorporated into the final product. The TREF result suggests that the grafting of the modifier to polyethylene has more likely occurred onto the chain backbone, rather than to the chain ends. This is because, only side chains in the polyethylene backbone will decrease TREF elution temperatures. Modifiers added to the polyethylene chain ends would not have a strong effect on the TREF elution temperature.

In this next study of two high impact polypropylene samples shown in Figure 21, the goal of the study is to find ways of modifying the features of company A polymer to mimic that of the company B product. From the 3D-GPC results, one sees that the company B product has higher molecular weight. But, there is still the question of not knowing where one needs to make a boost in molecular weight, whether it needs be in the rubber phase component or in the crystalline component of the company A product. The answer can

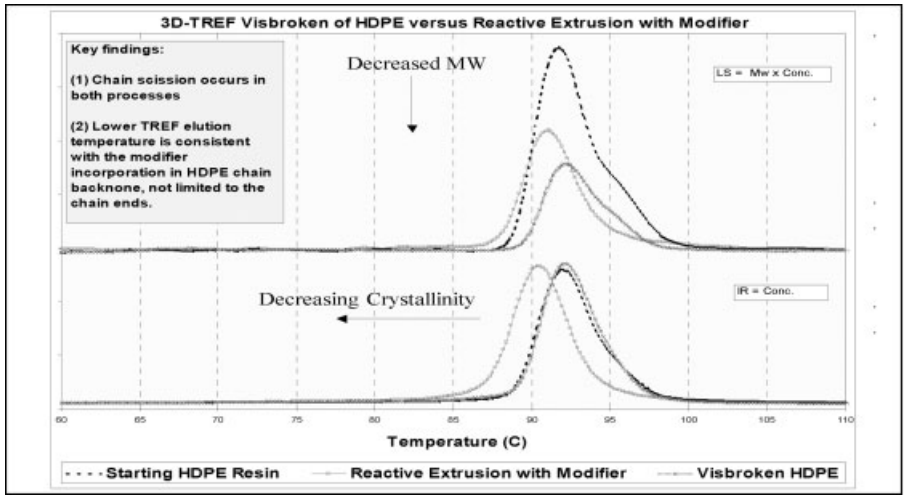


***Figure 20.***
3D-TREF study of HDPE visbreaking versus reactive extrusion with modifiers.

 

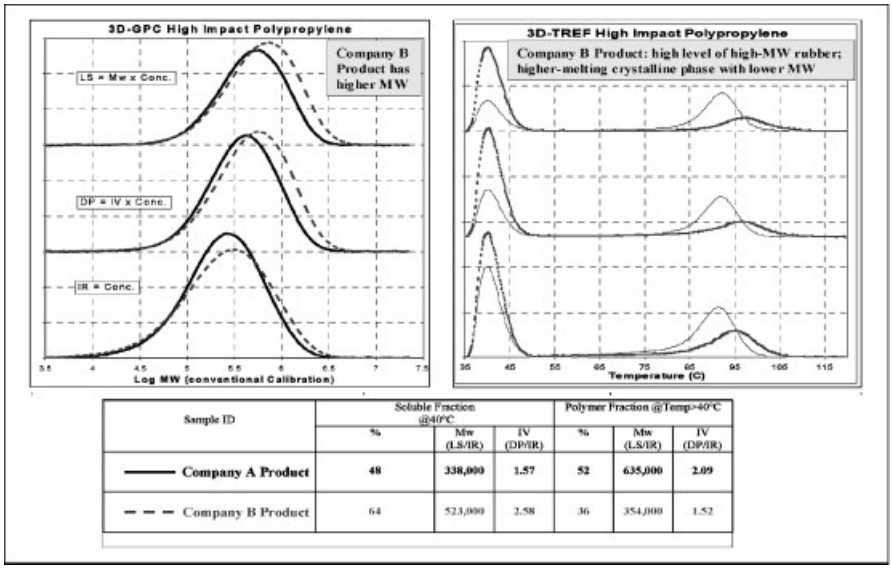


| Sample ID | Soluble Fraction @40°C | | | Polymer Fraction @Temp>40°C | | |
|---|---|---|---|---|---|---|
| | % | Mw (LS/IR) | IV (DP/IR) | % | Mw (LS/IR) | IV (DP/IR) |
| Company A Product | 48 | 338,000 | 1.57 | 52 | 635,000 | 2.09 |
| Company B Product | 64 | 523,000 | 2.58 | 36 | 354,000 | 1.52 |

***Figure 21.***
Reverse engineering of high-impact polypropylene using 3D-GPC-TREF.

be clearly seen in the 3D-TREF results of the two samples. The 3D-TREF result shows clearly that the increase in molecular weight needs to be in the rubbery component of the product. In fact, the molecular weight difference between the two products shown in the table at the bottom the Figure 21 also provides the information about how much increase of the rubber molecular weight is needed.

## Concluding Remarks

We found that the combination of 3D-GPC and 3D-TREF in a form of a hybrid system is a very powerful toll for studying polyolefin $\mu$-structures. Most of the successful applications of the technique in solving company problems are credited to a very large part to the high precision capability of our instrument. Automation of sample injection and temperature programming in our system is the key to our high precision analyses. Analytical information provided by this technique has the value to greatly shorten the product development time. Not only is 3D-GPC-TREF useful in understanding the $\mu$-structure of a given resin, it also has been useful in analyzing the composition of polymer blends and fabricated products. In today's challenging times in polyolefin industry, a strong program in 3D-GPC-TREF technology is a highly desirable element in a modern day polyolefin research organization.

*Acknowledgements:* The author wishes to acknowledge the technical assistance of Tia Kuhlman, Steve Elmore and Sue Setty for setting up and carrying out most of the 3D-GPC-TREF experiments during the course of this work.

[1] Waters Corporation, 34 Maple Street, Milford, MA 01757, USA.
[2] Polymer ChAR, Valencia Technology Park, P. O. Box 176 E-46980 Paterna, Spain. E-mail Info@polymerchar.com
[3] Precision Detectors, 34 Williams Way, P. O. Box 738, Bellingham, MA 02019, USA. E-mail Lighscatter@netscape.net
[4] Polymer Laboratories, Amherst Fields Research Park, 160 Old Farm Road, Amherst, MA 01002, USA. E-mail SalesUS@polymerlabs.com
[5] W. W. Yau, D. Gillespie, *Polymer* **2001**, *42*, 8947–8958; W. W. Yau, TAPPI 2005 PLACE Conference Proceedings, TAPPI PRESS, Atlanta, Session 19, Paper 19-1.

 

[6] W. W. Yau, TAPPI 2005 PLACE Conference Proceedings, TAPPI PRESS, Atlanta, Session 19, Paper 19-1; C. T. Enos, K. Rufener, J. Merrick-Mack, W. Yau, Waters International GPC Symposium Proceedings, June 6–12, **2003**, Baltimore, MD USA.
[7] R. Shroff, H. Mavridis, *Macromolecules* **1999**, *31*(25), 8454–8464.
[8] S. Anantawaraskul, J. B. P. Soares, P. M. Wood-Adams, *Macromol. Symp.* **2004**, *206*, 57–68; S. Anantawaraskul, J. B. P. Soares, P. M. Wood-Adams, *Journal of Polymer Sci.: Part B: Polymer Physics* **2003**, *41*, *1762–1778*.
[9] P. J. DesLauriers, D. C. Rohlfing, E. T. Hsieh, *Polymer* **2002**, *43*, 159–170.

 